Cell Stem Cell
Article

HIF-2α Protects Human Hematopoietic Stem/Progenitors and Acute Myeloid Leukemic Cells from Apoptosis Induced by Endoplasmic Reticulum Stress

Kevin Rouault-Pierre,[1,2,3,8] Lourdes Lopez-Onieva,[1,8] Katie Foster,[1] Fernando Anjos-Afonso,[1] Isabelle Lamrissi-Garcia,[2,3] Martin Serrano-Sanchez,[2,3] Richard Mitter,[4] Zoran Ivanovic,[3,5,6] Hubert de Verneuil,[2,3] John Gribben,[7] David Taussig,[7] Hamid Reza Rezvani,[2,3] Frédéric Mazurier,[2,3,9,*] and Dominique Bonnet[1,9,*]

[1]Haematopoietic Stem Cell Laboratory, London Research Institute, Cancer Research UK, WC2A 3LY, London, UK
[2]INSERM U 1035, Bordeaux, F-33076 France
[3]Université Bordeaux Segalen, Bordeaux, F-33076 France
[4]Bioinformatic and Biostatistic Department, London Research Institute, Cancer Research UK, WC2A 3LY, London, UK
[5]Établissement Français du Sang-Aquitaine Limousin, Bordeaux, F-33000, France
[6]CNRS UMR 5164, Bordeaux, F-33076 France
[7]Department of Haemato-Oncology, Barts Cancer Institute, Queen Mary University of London, London, EC1M 6BQ, UK
[8]These authors contributed equally to this work
[9]These authors contributed equally to this work
*Correspondence: mazurier@u-bordeaux2.fr (F.M.), dominique.bonnet@cancer.org.uk (D.B.)
http://dx.doi.org/10.1016/j.stem.2013.08.011

SUMMARY

Hematopoietic stem and progenitor cells (HSPCs) are exposed to low levels of oxygen in the bone marrow niche, and hypoxia-inducible factors (HIFs) are the main regulators of cellular responses to oxygen variation. Recent studies using conditional knockout mouse models have unveiled a major role for HIF-1α in the maintenance of murine HSCs; however, the role of HIF-2α is still unclear. Here, we show that knockdown of HIF-2α, and to a much lesser extent HIF-1α, impedes the long-term repopulating ability of human CD34$^+$ umbilical cord blood cells. HIF-2α-deficient HSPCs display increased production of reactive oxygen species (ROS), which subsequently stimulates endoplasmic reticulum (ER) stress and triggers apoptosis by activation of the unfolded-protein-response (UPR) pathway. HIF-2α deregulation also significantly decreased engraftment ability of human acute myeloid leukemia (AML) cells. Overall, our data demonstrate a key role for HIF-2α in the maintenance of human HSPCs and in the survival of primary AML cells.

INTRODUCTION

Multipotent hematopoietic stem cells (HSCs) reside in niches within the bone marrow (BM) and have a unique capacity to sustain life-long multilineage hematopoiesis (Li and Xie, 2005; Morrison and Spradling, 2008; Orkin and Zon, 2008; Scadden, 2006). It has been suggested that mammalian BM is relatively hypoxic compared to other tissues, with recent evidence suggesting that more primitive HSCs are localized in the most hypoxic microenvironment of the BM (Giuntoli et al., 2007; Kubota et al., 2008; Lévesque et al., 2007; Parmar et al., 2007). Within the stem cell niche, HSCs are maintained in a quiescent state with a low level of oxidative stress, which helps to prevent their differentiation and exhaustion (Jang and Sharkis, 2007).

The hypoxia-inducible factors (HIFs) are the main transcriptional factors responding to oxygen variation (Semenza, 2009a). HIF-1 and HIF-2 are heterodimeric proteins belonging to the basic helix-loop-helix. Regulation of HIF activity is mediated primarily through the stability of the alpha subunit. In normoxia, hydroxylation of the HIF-α protein leads to a decrease in the stability of HIF-α through rapid ubiquitination by the E3 ubiquitin ligase von Hippel-Lindau tumor suppressor protein (VHL) and degradation by the 26S proteosome. Under hypoxic conditions, HIF-α proteins are elevated as a result of reduced hydroxylation. The stabilized HIF-α subunit dimerizes with the HIF-1β subunit and activates the transcription of target genes involved in glucose metabolism, erythropoiesis, iron homeostasis, angiogenesis, and cell survival (Semenza, 2009a).

Additionally, under normoxic conditions, several factors such as thrombopoietin (TPO) and stem cell factor (SCF) have been shown to stabilize HIF-α subunits in hematopoietic cells (Kirito et al., 2005; Pedersen et al., 2008), suggesting an additional role for HIFs beyond that of responding to oxygen variations in the microenvironment.

In mice, the deletion of *Hif-1α* (Ryan et al., 1998) and *Hif-1β* (Adelman et al., 1999) results in embryonic lethality at E10.5, whereas the embryonic or perinatal lethality resulting from deletion of *Hif-2α* depends on the mouse microenvironment (Scortegagna et al., 2003a, 2003b). Recently, detailed analyses of the role of *Hif-1α* in adult mouse HSCs have been performed (Simsek et al., 2010; Takubo et al., 2010), demonstrating that the regulation of *Hif-1α* levels is critical for HSC maintenance in the hypoxic BM niche. Indeed, in *Hif-1α* -deficient mice, HSCs are less quiescent and their numbers decrease when exposed to various stressors (including BM transplantation, myelo-suppression, and aging) in a p16^{Ink4a}/p19^{Arf}-dependent manner. Further to this, the overstabilization of *Hif-1α* through biallelic loss of *Vhl*

induces cell cycle quiescence in HSCs and their progenitors and shows an impairment in their repopulating capacity, an effect similar to that observed in conditional knockouts of *cited2,* a competitor of Hif-1α for CBP/p300 (Kranc et al., 2009). Interestingly, monoallelic loss of *Vhl* also induces cell cycle quiescence yet improves BM engraftment after transplantation, suggesting that the regulation of the *Hif-1α* level is essential for mouse HSCs. Transcriptional activation of *Hif-1α* by Meis1 is reported to be involved in the anaerobic phenotype that characterizes HSCs in hypoxia (Simsek et al., 2010). Also, Miharada et al. have proposed a model by which *Hif-1α* induces Cripto/GRP78 signaling in the hypoxic HSC niche, which itself regulates the quiescence of HSCs by inducing a high level of glycolytic activity (Miharada et al., 2011). Overall, these studies have identified *Hif-1α* as a major regulator of mouse HSCs. With respect to *Hif-2α*, so far it has been shown to regulate *Epo* expression in the adult mouse (Gruber et al., 2007), contribute to tumor aggressiveness (Qing and Simon, 2009), and maintain the undifferentiated state of human neural crest-like neuroblastoma tumor-initiating cells (Pietras et al., 2009) and glioma-initiating stem cells (Li et al., 2009). *Hif-2α*$^{-/-}$ mice have also been reported to suffer multiple-organ pathology, including pancytopenia in the BM. Most importantly, Scortegagna et al. have suggested a central rheostat role for *Hif-2α* in both the maintenance of ROS levels and mitochondrial homeostasis (Scortegagna et al., 2003a, 2003b).

In contrast to the extensive work done in mice, at present what is known about the role of hypoxia and HIF-α in human HSC regulation remains limited. It has been reported that HIF-1α is expressed in Lineage^{-}CD34^{+}CD38^{-} cells from BM (Danet et al., 2003), as well as in circulating CD34^{+} and CD133^{+} cells under normoxic conditions (Piccoli et al., 2007). Furthermore, hypoxic ex vivo culture of BM cells or primitive hematopoietic progenitors has been shown to result in better maintenance of a primitive phenotype (Danet et al., 2003) and cell cycle quiescence (Hermitte et al., 2006). Mutations in *VHL*, *PHD*, or *HIF-2α* have been reported to lead to polycythemia in Chuvash's disease (Semenza, 2009b) through an increase in EPO production by the kidney and an increased sensitivity to EPO in these patients (Ang et al., 2002; Hickey et al., 2007).

HIF proteins have been also shown to be involved in cancer development, where high expression of HIF-α correlates with poor patient prognosis (Keith et al., 2012). A recent report suggests that HIF-1α is required for human leukemic stem cell (LSC) function in AML (Wang et al., 2011). However, the role of HIF-2α protein in human AML remains largely unknown.

In this work, we examine the effect of the knockdown (KD) of *HIF-1α* and *HIF-2α* in human HSPCs. We observe that silencing *HIF-2α*, and to a lesser degree *HIF-1α*, impedes the repopulating capacity of CD34^{+}-derived umbilical cord blood (UCB) cells in vivo. We demonstrate that HIF-2α KD HSPCs show signs of endoplasmic reticulum (ER) stress and activate the unfolded protein response (UPR) pathway, which ultimately affects the survival of the HSPCs. Moreover, we observe that the increase in the ER stress response in HIF-2α KD cells is due to an increase in reactive oxygen species (ROS) production. We also describe that cells from AML patient samples are dependent on the level of HIF-2α for their survival. Collectively, the data in our report provide further evidence of a central role for HIF-2α in protecting HSPCs and AML cells from apoptosis induced by ER stress.

RESULTS

The Expression of HIF-α Subunits in Human CD34^{+}Cells and Their Efficient KD Using shRNA Lentiviral Vectors

It has previously been shown that HIF-1α is expressed in Lin^{-}CD34^{+}CD38^{-} cells derived from the BM (Danet et al., 2003) and is present on peripheral blood cells (Piccoli et al., 2007). We first confirmed the expression of HIF-1α in freshly isolated CD34^{+} CB-derived cells and additionally demonstrated the expression of HIF-2α in these cells (Figure 1A). As expected, we were able to see an increase in HIF-1α and HIF-2α after incubating CD34^{+} cells with cobalt chloride ($CoCl_2$), which prevents the prolyl-hydroxylase activity leading to HIF degradation (Figure 1A) (Figure S1A available online).

To investigate the role of each of the HIF-α subunits in human HSPCs, we constructed bicistronic lentiviral vectors carrying two distinct promoters, EF1α and H1, driving green fluorescent protein (GFP) (reporter) and a small hairpin RNA (shRNA) against the *HIF-1α* (sequence published in Rezvani et al., 2007) or *HIF-2α* subunit, respectively (Figure S1B). To confirm the specificity and efficiency of these vectors, CD34^{+} cells were transduced (45%–80% transduction efficiency), FACS-sorted 4 days post-transduction, and cultured for an additional 4 days prior to our assessment of mRNA levels. A significant reduction in mRNA levels was observed for both *HIF-1α* and *HIF-2α* vectors relative to controls, with a decrease of 88% and 78%, respectively (Figure 1B). The KD was also confirmed at the protein level in CD34^{+} cells (Figure 1C) and in 293T cells (Figure S1C). The shHIF1α used in this study has been previously validated elsewhere (Rezvani et al., 2007). However, to confirm the specificity and exclude off-target effects of the shRNA for *HIF-2α*, we tested a second shHIF2α (shHIF2α.2) (Figure S1D). Using this second vector, we confirmed an efficient KD at the protein level, as well as similar defects in vivo compared to the first shRNA used (shHIF2α.1) (Figure S1E). We then used the construct that gave us the best silencing activity (shHIF2α.1) for the rest of this study.

To further confirm the specificity of our shRNA vectors, we looked at the effect of the KD on known target genes of HIF-1α (*VEGFA* and *LDHA*) and HIF-2α (*VEGFA* and *HES-1*). We observed a significant reduction of *VEGFA* expression after both *HIF-1α* and *HIF-2α* silencing, a reduction of *LDHA* following HIF-1α KD, and a reduction of *HES-1* after HIF-2α KD (Figure 1D), indicating that our shRNA vectors were specific.

Silencing *HIF-2α* and, to a Lesser Extent, *HIF-1α*, Affects Human Short-Term Repopulating Cells

It has been reported that the formation of myelo-erythroid progenitors from embryonic or yolk sac cells derived from *Hif-1α*-, *Hif-2α*-, and *Hif-1β*-knockout mice is impaired (Adelman et al., 1999; Covello et al., 2006; Yoon et al., 2006). However, no major impediment to the in vitro functions of adult mouse HSCs has been observed using a conditional knockout model of *Hif-1α* (Takubo et al., 2010). We therefore examined the effect of HIF-α KD in human hematopoietic progenitor cells. The number of myeloid colonies generated from GFP^{+} cells was equivalent in

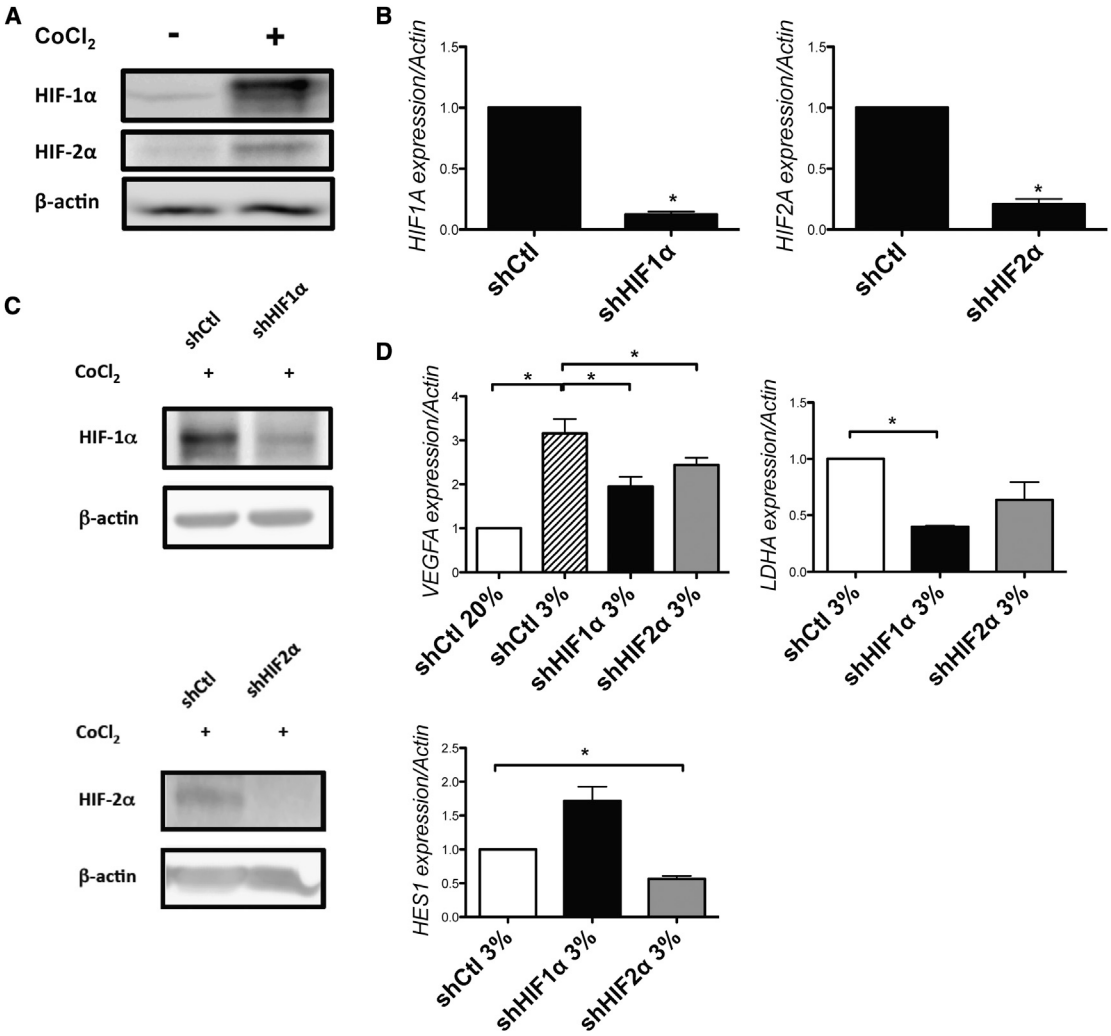

Figure 1. Expression of HIFα Subunits in Human CD34$^+$ Cells and Their Efficient KD Using shRNA Lentivirus Vectors

(A) HIF-1α and HIF-2α protein expression in freshly purified CD34$^+$ cells cultured for 6 hr in the presence or absence of $CoCl_2$.

(B) RT-QPCR for *HIF-1α* (left) and *HIF-2α* (right) expression in CD34$^+$ cells. CD34$^+$ cells were transduced with shCtl, shHIF1α, and shHIF2α, and sorted on day 4 posttransduction based on GFP$^+$. Gene expression was normalized to *B-ACTIN* gene and then to the shCtl (n = 3). Results are shown as the mean ± SEM. *p < 0.05.

(C) HIF-1α (upper) and HIF-2α (lower) protein expression in CD34$^+$ cells after transduction. CD34$^+$ cells were transduced with shCtl, shHIF1α, and shHIF2α, and sorted on day 4 posttransduction based on GFP$^+$ cells and cultured for another 6 hr in the presence of $CoCl_2$ before protein extraction and western blot analysis.

(D) RT-QPCR for *VEGFA* (common target gene for HIF-1α and HIF-2α), *LDHA* (HIF-1α target gene), and *HES-1* (HIF-2α target genes) expression in CD34$^+$ transduced cells cultured at 20% and 3% of oxygen. RT-PCR was normalized to *B-ACTIN* and data are expressed relative to shCtl at 3% oxygen (n = 3–5). Results are shown as the mean ± SEM. *p < 0.05.

See also Figure S1.

all conditions (Figure 2A). However, the number of erythroid colonies was significantly diminished upon HIF-2α KD, where there was a 61% reduction compared to the control. No effect was observed in HIF-1α silenced cells (Figure 2A). Further analysis of the effect of HIF-2α KD on erythropoiesis is being investigated (data not shown).

To determine whether HIF-α KD has an effect on the proliferation of CD34$^+$ cells, we performed a short-term liquid culture assay in the presence of growth factors. Under these conditions, we showed that silencing *HIF-2α* significantly reduced the proliferation of CD34$^+$ cells (Figure 2B); however, no change was seen when *HIF-1α* was silenced. This effect on proliferation was not due to an increase in apoptosis (Figure 2C). Thus, under normoxic conditions, only the downregulation of HIF-2α had an effect on CD34$^+$ cells, reducing both erythroid colony formation and proliferation.

We further examined the effect of HIF-α silencing in vivo using the NOD-SCID/IL2Rg^{null} (NSG) xenotransplantation model, as depicted in Figure 2D (left panel). Immediately after transduction, cells were injected intravenously into mice and human graft was examined 6 weeks posttransplantation. The percentage of GFP$^+$ cells within the human CD45$^+$ fraction was determined by flow cytometry. A loss of transduced cells was observed in both HIF-1α and HIF-2α KD conditions, although this effect was less

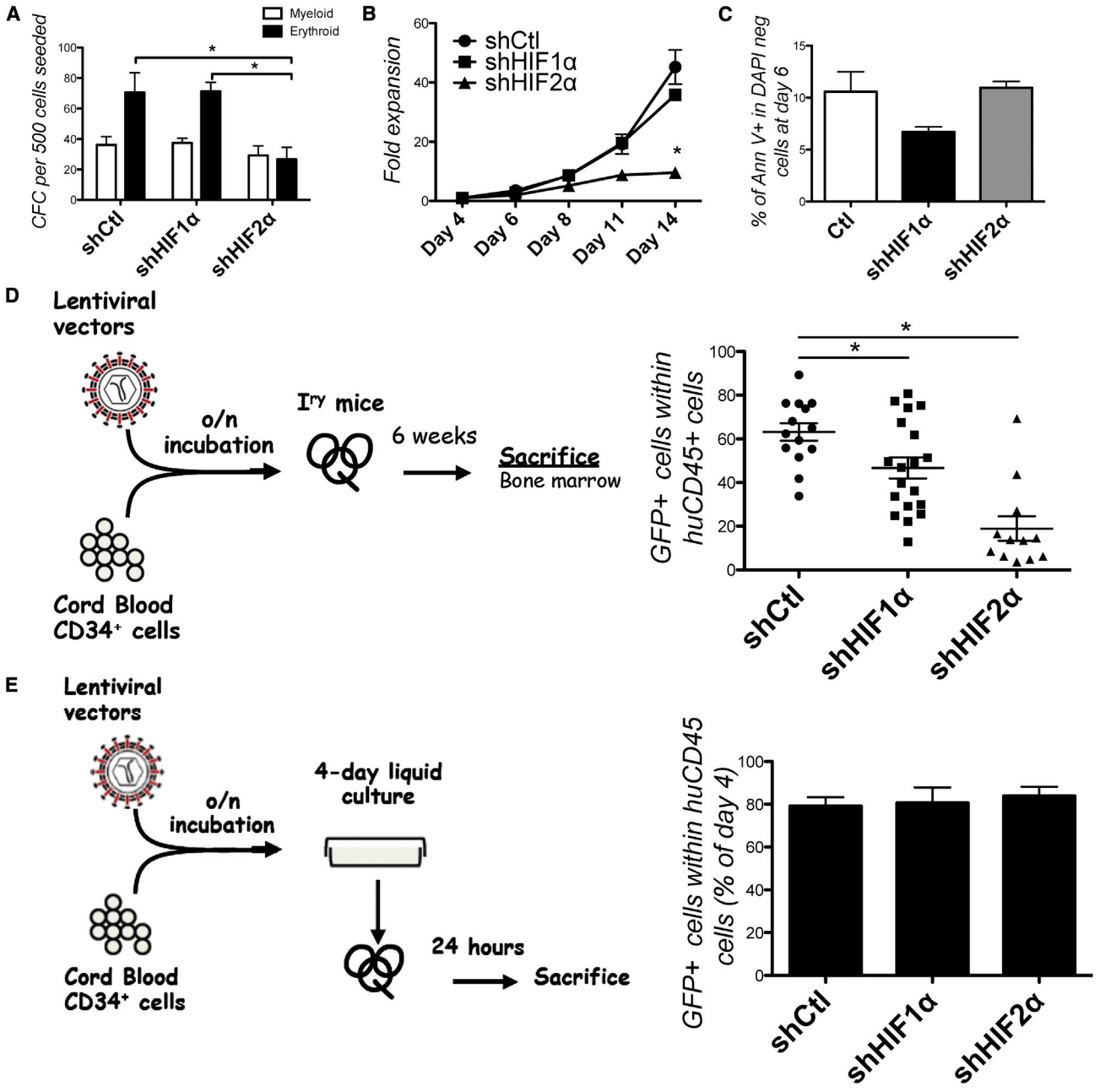

Figure 2. HIF-1α and HIF-2α KDs Differently Affect Human Progenitor Compartment

(A) Colony forming unit (CFU) assay of $CD34^+$ cells transduced with shCtl, shHIF1α, or shHIF2α. Five hundred $CD34^+$ GFP^+ transduced cells were plated. Two weeks later the number of colonies was determined (n = 3).

(B) $CD34^+$ transduced and sorted cells were grown in expansion medium and the number of cells was determined every 2–3 days. The growth curve represents cumulative cell numbers (n = 3).

(C) Early apoptosis was assessed on transduced $CD34^+$ cells after 6 days in liquid culture. Data represents the percentage of Annexin V^+ cells in the $DAPI^-$ population (n = 3).

(D) Left panel, schematic of the in vivo short-term repopulation assay. $CD34^+$ cells were transduced with shCtl, shHIF1α, and shHIF2α and then injected into NSG mice. Human graft was determined 6 weeks posttransplantation. Right panel, percentage of GFP^+ cells in the human engraftment. Results are shown as normalized to 100% GFP^+ at day 4. Results represent three to six independent experiments and each dot represents one mouse.

(E) Left panel, schematic of the homing assay. $CD34^+$ cells were transduced with shCtl, shHIF1α, and shHIF2α and then injected into mice. Human graft was determined 24 hr after transplantation. Right panel, percentage of GFP^+ cells. Results are shown as normalized to 100% GFP at day 4. Graph represents two independent experiments (n = 6 mice per bar).

Results in (A), (B), and (D) are shown as mean ± SEM. *$p < 0.05$.

pronounced in HIF-1α KD cells (up to 26% loss compared to the value at day 4) than that in HIF-2α KD (up to 70%; see Figure 2D, right panel).

Hypoxia and HIFs have been described as important factors driving the expression of the chemokine SDF-1α (Ceradini et al., 2004) and its receptor, CXCR4, in tumors (Liu et al., 2006). Based on the role of SDF-1α and CXCR4 in human stem cell homing and repopulation (Lapidot and Kollet, 2002), we hypothesized that the KD of both HIF-α subunits might affect the homing of transduced cells. To test this hypothesis, we transduced $CD34^+$ cells and kept these cells in liquid culture for 4 days prior to injection into mice (see schematic protocol, Figure 2E, left panel). Mice were sacrificed 24 hr after injection and human hematopoietic cell homing was determined by the percentage of GFP-expressing cells among human cells (Figure 2E, right panel). The percentage of GFP-expressing cells within human grafts was not significantly different between the three groups (shCtl, shHIF1α, and shHIF2α), suggesting that there is no homing defect that occurs upon the silencing of the HIF-α subunits.

HIF-2α KD Impairs the Long-Term Reconstitution Ability of Human HSPCs

Using a conditional knockout mouse model, it was recently shown that *Hif-1α* is required to sustain long-term hematopoietic repopulation capacity under stress conditions (Takubo et al., 2010), whereas *Hif-2α* knockout only causes a minor effect in the primitive hematopoietic compartment (Scortegagna et al., 2003a). To investigate the role of HIF-α in the long-term maintenance of human HSPCs, we followed the percentage of GFP^+ cells in transplanted NSG mice over time by BM aspiration sampling at 3, 6, 12, and 24 weeks (at the time of sacrifice) after transplantation, as described in Figure 3A. A progressive decrease in the percentage of GFP^+ cells in the first 12 weeks was observed in mice transplanted with shHIF1α-transduced cells as compared to the control condition (shCtl) (Figure 3B), an effect that plateaued after 12 weeks. A more dramatic drop in the first 12 weeks was observed upon transplantation of shHIF2α-transduced cells (Figure 3B), which persisted until 24 weeks. A similar decrease in the myeloid ($CD33^+$) and lymphoid ($CD19^+$) compartments was observed in both shHIF1α and shHIF2α cells (Figure 3C), suggesting that in both cases, silencing affected immature HSPCs. To demonstrate that the decrease was not due to a change in the distribution of the cells in the different hematopoietic tissues, we checked the engraftment of transduced cells in the BM, peripheral blood (PB), and spleen of these mice (Figure 3D). We observed the same decrease in engraftment in each of the different tissues, affecting both myeloid and lymphoid compartments (Figure 3E).

Because *HIF-2α* KD cells showed a significant decrease in reconstitution 3 weeks after injection, we wondered whether this might be due to a defect in the retention and/or anchorage of the cells in their niche. To assess this question we examined the effect of *HIF-2α* silencing on engrafted cells 1 and 2 weeks after transplantation. One week posttransplantation, we did not observed any loss of transduced cells in the *HIF-2α* KD as compared to controls. However, 1 week later, a mild but significant reduction in engraftment was detected (Figure S2A). These results suggest that HIF-2α does not play a major role in the retention of the HSCs in their niches. We confirmed this by tracking HSCs in their niches using noninvasive intravital microscopy of the calvaria. For this purpose, $CD34^+CD38^-$ HSPCs were transduced and sorted 4 days later based on GFP expression. Cells were then stained with CFSE and injected into mice as schematically depicted (Figure S2B, left panel). Based on unpublished data from our group, we have observed that after 4 days posttransplantation, HSCs have reached their niches (K. Foster, F. Lassailly, F. Anjos-Afonso, E. Currie, and D.B., data not shown). At this stage, we can thus measure the distance of each HSPC to the closest endothelial cells or endosteal region. Using these measurements, we did not observe any difference in the positioning of HSPCs between control and *HIF-2α* KD (Figure S2B, right panel). These results confirmed that HIF-2α silencing has no effect on the HSC lodgement/retention in their niches in the first week posttransplant.

To evaluate the effect on the most primitive compartment, we compared the percentage of $CD34^+CD38^-$ cells present in the BM of these mice 24 weeks posttransplant. We observed a slight but significant decrease in the $CD34^+CD38^+$ HPC fraction and a nonsignificant decrease in the $CD34^+CD38^-$ HSPC compartment in shHIF1α transplanted mice. This was in contrast to a 90% reduction in both subfractions in the shHIF2α-silenced group, suggesting a key role for *HIF-2α* in the human HSPC compartment (Figure 3F).

To address the impact that each of the HIF-α subunits could have on the self-renewal capacity of human HSPCs, we went on to perform secondary transplantations. Mice were injected with a pool of BM cells from the primary grafts and sacrificed 24 weeks posttransplant. Based on the low percentage of GFP^+ cells retrieved from the shHIF2α group, we were only able to inject 6 mice, as compared to 16 mice in the shHIF1α group. Nevertheless, a further 48% reduction in the percentage of shHIF-2α transduced cells was observed at 24 weeks postsecondary transplantation as compared to the level obtained at 24 weeks postprimary transplantation; once again, in contrast, no further reduction was observed with shHIF1α cells (Figure 3G). This data strongly demonstrates that the maintenance of human long-term repopulating cells with self-renewing ability is dependent on HIF-2α. Recently, Kocabas et al. described that *Hif-1α*$^{-/-}$ long-term HSCs show a compensatory upregulation of *Hif-2α* mRNA (Kocabas et al., 2012). Similarly, we have observed that the KD of HIF-1α in human $CD34^+$ cells cultured for 4 days under hypoxia (3% O_2) or normoxia (20% O_2) (data not shown) results in a 3-fold increase in *HIF-2α* mRNA levels (Figure S2C). This was further confirmed by the increase in expression of *HES-1*, a downstream target of HIF-2α (Figure 1D). This marked compensatory upregulation of *HIF-2α* in shHIF1α-transduced cells could explain why no significant long-term effect was observed on shHIF1α HSPCs.

The HIF pathway is a well-established regulator of the cell cycle. In order to determine if the dramatic effect that *HIF-2α* silencing had on HSPCs was due to a defect in proliferation, we performed cell cycle analysis on engrafted cells 1 and 2 weeks after injection. No differences in any phases of the cell cycle were observed in the absence of HIF-2α, suggesting that the effect observed is independent of cell cycle (Figure S2D).

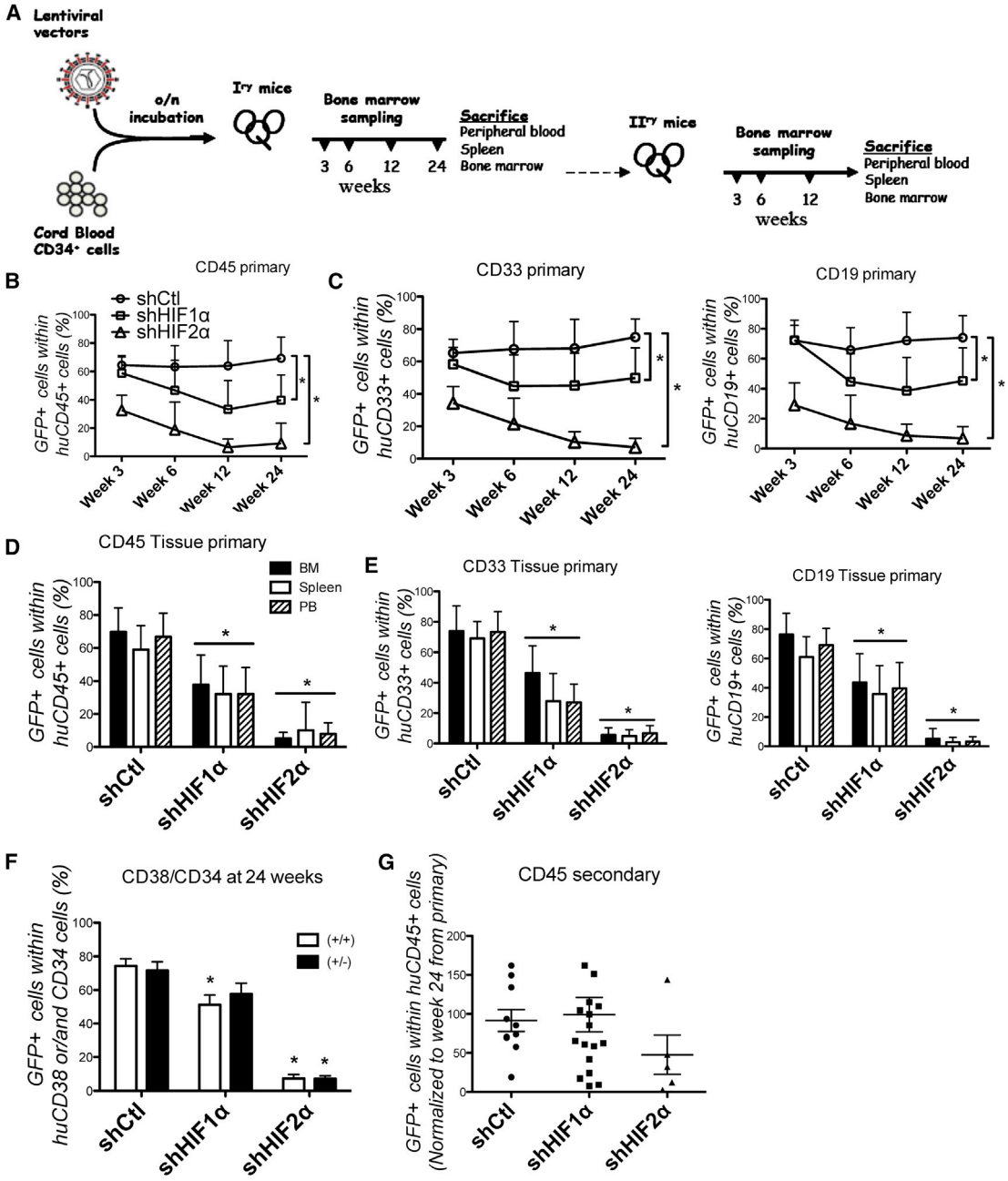

Figure 3. HIF-2α Is Essential for the Long-Term Engraftment Ability of the Human Hematopoietic Cells in NSG Mice

(A) Schematic representation of the in vivo primary and secondary transplantation assay and BM sampling at different time points. Results represent three to six independent experiments and total number of mice are as follows: shCtl, n = 14; shHIF-1α, n = 19; shHIF-2α, n = 12.

(B) In vivo kinetic of transduced cells in human hematopoietic population. Percentages of GFP$^+$ cells in total human CD45$^+$ cells at the indicated time are shown. Results are shown as normalized to 100% GFP at day 4 as mean ± SD. *p < 0.05.

(C) In vivo kinetic of transduced myeloid and lymphoid population. Percentages of GFP$^+$ cells in total CD33$^+$ (left panel) and in total CD19$^+$ cells (right panel) at the indicated time are shown. Results are shown as normalized to 100% GFP at day 4 as mean ± SD. *p < 0.05.

(D and E) Twenty-four weeks after transplantation mice were sacrificed and the percentage of GFP$^+$ cells in bone marrow (BM), spleen, and peripheral blood (PB) was analyzed. (D) GFP$^+$ cells in total CD45$^+$ human cells. (E) Left panel, as in (D), but in total CD45$^+$CD33$^+$-myeloid cells; right panel, as in (D), but in total CD45$^+$CD19$^+$-B-lymphoid cells. Results are shown as mean ± SD. *p < 0.05.

(F) Twenty-four weeks after the first transplantation, mice were sacrificed and the percentage of GFP$^+$ cells in CD34$^+$CD38$^{lo/-}$ and CD34$^+$CD38$^+$ populations was analyzed by FACS. Results are shown as mean ± SEM. *p < 0.05.

(G) BM from primary animals was injected into secondary mice. Twenty-four weeks later, percentages of GFP$^+$ cells within the human graft were analyzed by FACS. Results are shown as normalized to 100% GFP at week 24 as mean ± SEM. Each dot represents a mouse.

See also Figure S2.

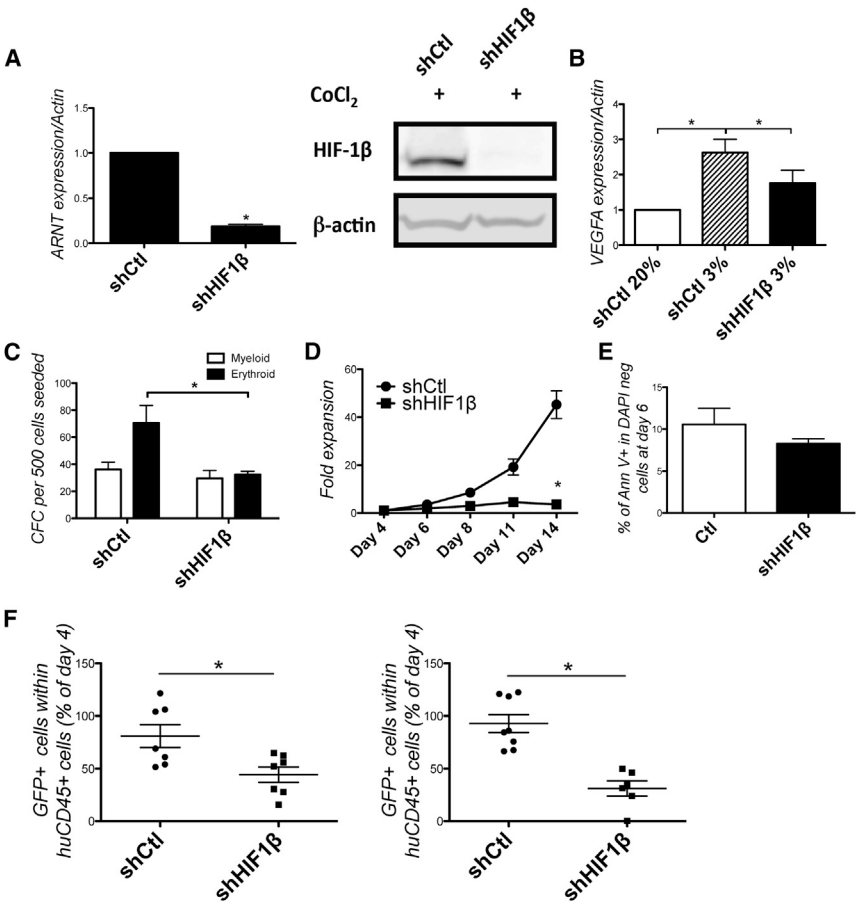

Figure 4. HIF-1β KD in CD34⁺ Cells Recapitulates HIF-2α KD Phenotype

(A) Left panel, RT-QPCR for *HIF-1β* expression in CD34⁺ cells transduced with shCtl or shHIF1β (n = 3). Right panel, HIF-1β protein expression in CD34⁺ cells transduced with shCtl or shHIF1β and cultured for 6 hr in presence of $CoCl_2$.

(B) RT-QPCR for *VEGFA* expression in CD34⁺ transduced cells cultured at 20% and 3% of oxygen. *B-ACTIN* was used as a housekeeping gene (n = 3).

(C) CFU assay of CD34⁺ cells transduced with shCtl and shHIF1β. Five hundred GFP⁺ CD34⁺ were plated and 2 weeks later numbers of colonies were determined (n = 3).

(D) CD34⁺ transduced cells were grown in expansion medium and the number of cells was determined every 2–3 days. The growth curve represents cumulative cell numbers (n = 3).

(E) Early apoptosis was assessed on CD34⁺ transduced cells after 6 days in liquid culture. Data represents the percentage of Annexin V⁺ cells in the DAPI⁻ population (n = 3).

(F) Mice were transplanted with CD34⁺ cells transduced with either shCtl or shHIF1β. Six weeks (left panel) or twelve weeks (right panel) after transplantation mice were killed and the percentage of GFP⁺ cells in the human engraftment was analyzed. Results are shown as normalized to 100% GFP at day 4. Results represent two independent experiments and each dot represents one mouse.

Results are shown as mean ± SEM. *p < 0.05.

HIF-1β KD in CD34⁺ Cells Recapitulates the HIF-2α KD Phenotype

To better understand the role of HIF-α in HSPCs, we decided to knock down the binding partner of the HIF-α subunits, the constitutively expressed β subunit (HIF-1β). We confirmed the downregulation of HIF-1β using an shHIF1β at both mRNA and protein level (Figure 4A, left and right panels), and by noting the decrease in the downstream target gene *VEGFA* (Figure 4B).

We examined the effect of the downregulation of HIF-1β on progenitor formation, cell proliferation, and apoptosis. We observed a specific decrease in erythroid progenitors (Figure 4C) and cell proliferation (Figure 4D) without a change in the level of apoptosis (Figure 4E). These results closely overlap with the effects seen in HIF-2α KD. The similarity in the effect of HIF-1β and HIF-2α KD in HSPCs was further confirmed in vivo, at both 6 (Figure 4F, left panel) and 12 weeks (Figure 4F, right panel) posttransplant, where a significant decrease in engraftment was seen at both time points, confirming the role of HIF complexes in the maintenance of human HSPCs.

HIF-2α KD Increases ROS Production and Affects Mitochondrial Homeostasis

Because our results suggested that HIF-2α plays an important role in the maintenance of human long-term self-renewing repopulating stem cells, we decided to focus our efforts on understanding the molecular mechanisms by which HIF-2α regulates HSPC biology. To investigate this, human CD34⁺ cells transduced with shHIF2α were recovered from mouse BM 6 weeks posttransplantation and subjected to a large-scale gene expression analysis after we first confirmed the efficiency of *HIF-2α* silencing at this time point (61% silencing efficiency at the mRNA level; Figure S3A). Compared to shCtl-transduced cells, gene pathway enrichment analysis identified the oxidative stress, ER stress response, and apoptosis pathways as those with the largest change in gene signature (Figure 5A, left panel).

Based on the gene expression signature for the oxidative stress pathway observed in shHIF2α cells, and the known role of HIF-2α in regulating reactive oxygen levels (Scortegagna et al., 2003a, 2003b), we examined the level of ROS present in these cells both in vitro and at 6 weeks posttransplantation. As hypothesized, ROS levels were significantly increased in liquid culture (Figure S3B) and in all compartments ($CD34^+CD38^-$, Lin^+ cells and a trend in $CD34^+CD38^+$ cells) in vivo after transduction with shHIF2α as compared to shCtl (Figure 5B).

Mitochondria are a major source of ROS and mechanisms to prevent elevated ROS during oxidative phosphorylation require the activity of antioxidant enzymes. Recently, it was shown that HIF-2α regulates the expression of genes encoding antioxidant enzymes in mice (Bertout et al., 2009; Gordan et al., 2007). Based on the increase in ROS, we examined the level of expression of antioxidant genes, such as superoxide dismutase 2 (*SOD2*), as well as genes involved in mitochondria homeostasis,

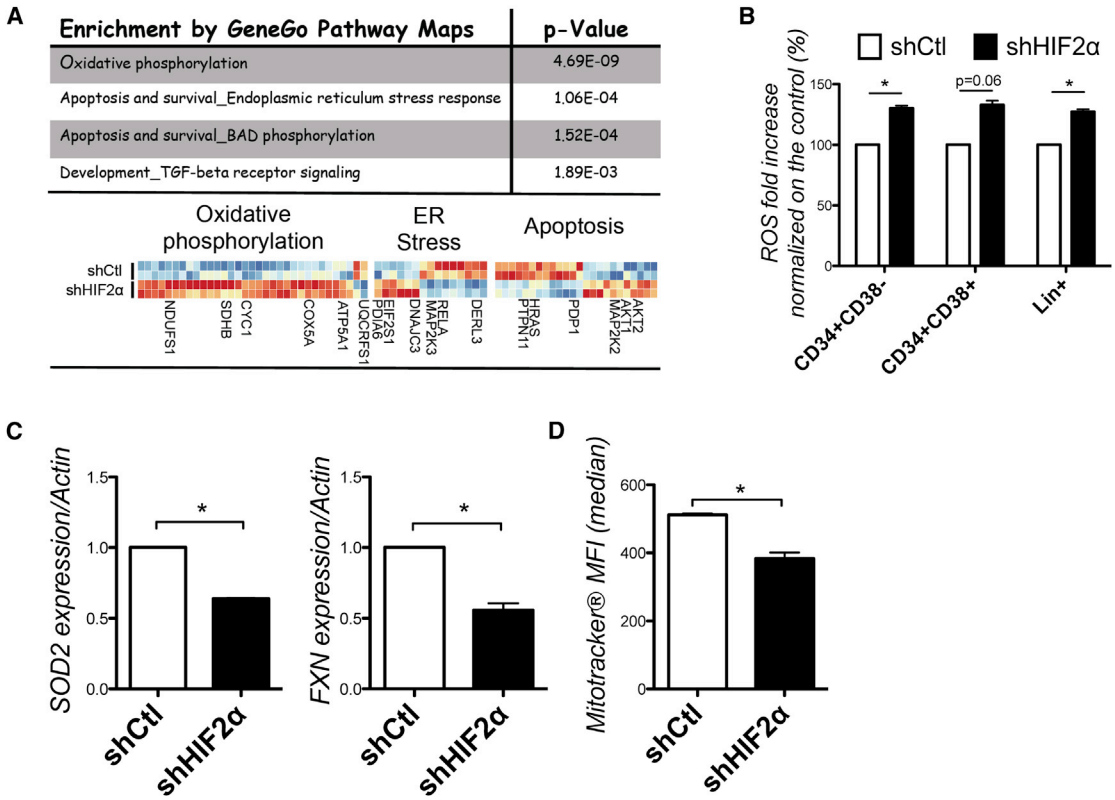

Figure 5. HIF-2α KD In Vivo Increases ROS Production and Affects Mitochondria Homeostasis

(A) Large-scale gene expression on human CD34$^+$ GFP$^+$ cells sorted from mice at 6 weeks. Gene pathway enrichment analysis ranked on top position the oxidative phosphorylation pathway, ER stress response, and apoptosis and survival. A heat-map is presented below for two different mice in each condition (shCtl and shHIF-2α).

(B) In vivo quantification of ROS in shCtl and shHIF2α in Lin$^-$CD34$^+$CD38$^{lo/-}$, Lin$^-$CD34$^+$CD38$^+$, and Lin$^+$ cells 6 weeks posttransplantation. Data is presented as percentage of ROS increase in shHIF2α compared to the shCtl (normalized to 100%). ShCtl, n = 5 mice; shHIF2α, n = 11 mice. Results are shown as the mean ± SEM. *p < 0.05.

(C) RT-QPCR for *SOD2* (left) and *FXN* (right) expression in CD34$^+$ cells transduced with shCtl or shHIF-2α. Transduced cells were sorted for GFP$^+$ on day four and cultured for an extra 7 days under 3% of oxygen. *B-ACTIN* was used as control (n = 3). The results are expressed in comparison to the level in shCtl. Results are shown as the mean ± SEM. *p < 0.05.

(D) Mean fluorescence intensity (MFI) of MitoTracker-stained CD34$^+$ cells transduced with shCtl or shHIF2α. (n = 3). Results are shown as mean ± SEM. *p < 0.05. See also Figure S3.

such as Frataxin (*FXN*). A significant decrease in both genes was observed in shHIF2α transduced CD34$^+$ cells compared to shCtl (Figure 5C). We also looked at the alterations in mitochondrial membrane potential and oxidant stress by performing MitoTracker staining. We observed a significant decrease in the mean fluorescence intensity of MitoTracker-stained CD34$^+$ cells transduced with shHIF2α compared to control cells. Taken together, these data suggest that HIF-2α KD increases ROS production and affects mitochondria homeostasis (Figure 5D).

Silencing HIF-2α Increases the ER Stress Induced by ROS

As mentioned above, our large-scale gene expression analysis also identified the apoptosis-ER stress response pathway as one of the top ranked pathways differentially expressed in shHIF2α transduced CD34$^+$ cells compared to shCtl. Upon ER stress, UPR is activated through three distinct signaling pathways that regulate the expression of genes responsible for the maintenance of cellular homeostasis: the protein kinase R (PKR)-like ER kinase (PERK), the activating transcription factor 6 (ATF6), and the inositol-requiring protein 1a (IRE1α) signaling transducer pathways (Figure 6A). If ER stress persists and homeostasis is not restored, UPR signaling induces apoptosis (Walter and Ron, 2011). Interestingly, factors such as oxidative stress can induce ER stress (Malhotra and Kaufman, 2007).

To confirm the involvement of the ER stress response and the induction of the UPR pathway in HIF-2α KD HSPCs, we examined the expression levels of two ER chaperones, *HSPA5* (also known as 78 kDa glucose regulated protein, *GRP78*) and 94 KDa glucose regulated protein (*GRP94*). These genes have been widely used as sentinel markers of ER stress and UPR pathway activation. Human transduced GFP$^+$CD34$^+$ cells were sorted at day 4 posttransduction and cultured for an additional day before RNA was extracted and RT-PCR was performed. Upon HIF-2α KD, we observed an increase in both *HSPA5* and *GRP94* as compared to control (Figure 6B). We also observed a mild increase in C/EBP homologous protein (*CHOP*), a target gene of the PERK pathway that is expressed under ER

stress-induced cell apoptosis (Figure 6B). To further confirm the initiation of the UPR pathway by ER stress, we treated our cells with tunicamycin (TM), a well-known inducer of the UPR pathway. After their treatment with TM, we observed a significant increase in *HSPA5*, growth arrest and DNA damage inducible 34 gene (*GADD34*), and *CHOP*, which are key players of the PERK branch of the UPR pathway, in shHIF2α cells compared to the shCtl (Figure 6C, left panel). We also observed that the treatment with TM increased the percentage of apoptotic cells in shHIF2α cells compared to shCtl (Figure 6C, right panel). Taken together, these data suggest that HIF-2α-silenced HSPCs have significantly increased levels of ER stress and are more susceptible to apoptosis as a result. We further confirmed the activation of the PERK signaling pathway in these cells by looking at the eIF2α phosphorylation. Indeed P-eIF2α was higher in the *HIF-2α* KD cells compared to the control while the total eIF2α protein level remained the same (Figure 6D, left panel, and Figure S4A). We also assessed the activation status of the other two branches of the UPR pathway. No activation of the ATF6 branch was observed in *HIF-2α* KD cells as evidenced by the low or nondetectable expression of the activated, nuclear form of ATF6 ($ATF6_{50}$) in both shCtl and shHIF2α cells (Figure S4B). Additionally, we checked the activation of the IRE-1 pathway by measuring the mRNA splicing of the *XBP-1* transcription factor, which is a substrate of the IRE-1 activated form. We observed similar expression levels of the spliced *XBP1* mRNA in both control and *HIF-2α* KD cells (Figure S4C), suggesting that this branch is constitutively activated regardless of HIF-2α levels. These data suggest that HIF-2α silencing in HSPCs triggers ER stress mainly through the activation of the PERK branch of the UPR signaling cascade.

Finally, we confirmed the activation of the pathway in cells retrieved from mice 6 weeks posttransplant. We observed an upregulation of the downstream targets of p-eIF2α, such as *HSPA5*, *CHOP*, and *GADD34* (the latter two activated in response to prolonged ER stress), and a downregulation of *BCL-2* (an antiapoptotic gene that acts downstream of CHOP) in *HIF-2α* KD cells compared to shCtl cells (Figure 6E).

To further confirm the presence of ER stress, we performed electron microscopy on *HIF-2α* KD $CD34^+$ cells after they underwent 6 days in liquid culture. Electron microscopy identifies features of ER stress, shown by ER dilatation in the *HIF-2α* KD cells compared to control cells (Figure 6D, right panel).

Considering the increase in both ROS production and ER stress levels in HIF-2α KD cells, we wondered whether the increase in ROS could trigger the activation of the UPR pathway, ultimately leading to a decrease in the survival of the HSPCs and therefore a decrease in engraftment in vivo. To answer this question, we use GFP^+ $hCD45^+$ cells obtained from the BM of transplanted mice (6 weeks posttransplant) and pretreated these cells ex vivo with N-Acetyl-L-cysteine (NAC) or 4-Hydroxy-TEMPO (TEMPOL), two potent antioxidants, for 24 hr, followed by an additional treatment with TM for 24 hr (Figure 6F). We measured the level of apoptosis using Annexin V/DAPI staining before and after TM treatment. We observed that shHIF2α transduced cells were more susceptible to apoptosis under TM treatment compared to shCtl cells (Figure 6G). Furthermore, we were able to rescue the apoptosis caused by TM by pretreating the cells with either NAC or TEMPOL, after which significantly fewer apoptotic cells were observed (Figure 6H). To further confirm the activation of the UPR pathway through the loss of control of ROS production, we attempted to rescue the engraftment defect observed in HIF-2α-silenced cells by treating mice engrafted with shCtl- or shHIF2α-transduced cells with either NAC or TEMPOL every other day for 6 weeks. As shown in Figure 6I, treatment with TEMPOL, and to a lesser extent, NAC, was successful at rescuing the engraftment defect caused by HIF-2α silencing.

From this, our data suggest a pathway by which HIF-2α protects human HSPCs from ROS-induced ER stress and UPR pathway activation.

HIF-2α KD Impedes the Growth of Human Primary Acute Myeloid Leukemia

In solid tumors, the expression of *HIF-2α* has been associated with poor prognosis (Qing and Simon, 2009). We therefore decided to investigate the effect of the KD of HIF-2α on human primary acute myeloid leukemia (AML). First, we compared the level of expression of *HIF-2α* between $CD34^+$ cells from normal adult BM and 35 primary AML samples (33 samples at diagnosis and 2 samples at both diagnosis and relapse). We observed a large variability in *HIF-2α* levels in the AML samples tested, which could be related to AML subtypes and genomic abnormalities. Nevertheless, mean expression levels in AML were not significantly different as compared to normal BM (Figure 7A). We went on to evaluate the effect of HIF-2α KD on six AML samples (Patient 3 being tested at diagnosis and relapse) in ex vivo long-term culture. We saw a significant decrease in the percentage of GFP^+ cells over 3 weeks compared to shCtl in all samples tested ($p < 0.007$) (Figure 7B). We confirmed that *HIF-2α* mRNA was efficiently silenced (75%) in the HIF-2α KD AML samples compared to that in controls after 3 weeks in ex vivo cultures (Figure S5A).

Next, we went on to test the effect of this silencing in vivo in six AML patient samples (Patient 3 being tested at diagnostic and relapse). We observed an overall significant reduction ($p < 0.001$) in the engraftment of shHIF2α transduced cells, and in two cases, a complete abolition of the engraftment of the leukemia (Figure 7C). Of note, for Patient 3, we observed a more potent inhibition of the engraftment from the relapse sample, suggesting no acquisition of resistance mechanisms. To demonstrate that this effect on engraftment involves the UPR pathway, we treated AML cells ex vivo with TM and observed an increase in apoptosis in shHIF2α transduced cells compared to shCtl (Figure S5B). This suggests that HIF-2α KD cells were more susceptible to apoptosis as a result of ER stress. We also examined the expression levels of *HSPA5*, *CHOP*, and *GADD34* on these AML patient samples and observed a clear upregulation of these target genes under ER stress (Figure 7D).

Finally, to investigate if ROS was triggering apoptosis through the UPR pathway, we pretreated the AML cells ex vivo with NAC for 24 hr, followed this with an additional treatment with TM for 24 hr, and measured the level of apoptosis after treatment (Figure 7E). Similar to what we observed in HSPCs, we were able to rescue the apoptosis caused by TM by pretreating the cells with NAC, as significantly fewer apoptotic cells were observed (Figure 7F).

These data further indicate that HIF-2α is not only important for the maintenance of human normal HSPCs, but is also active in primary AML cells.

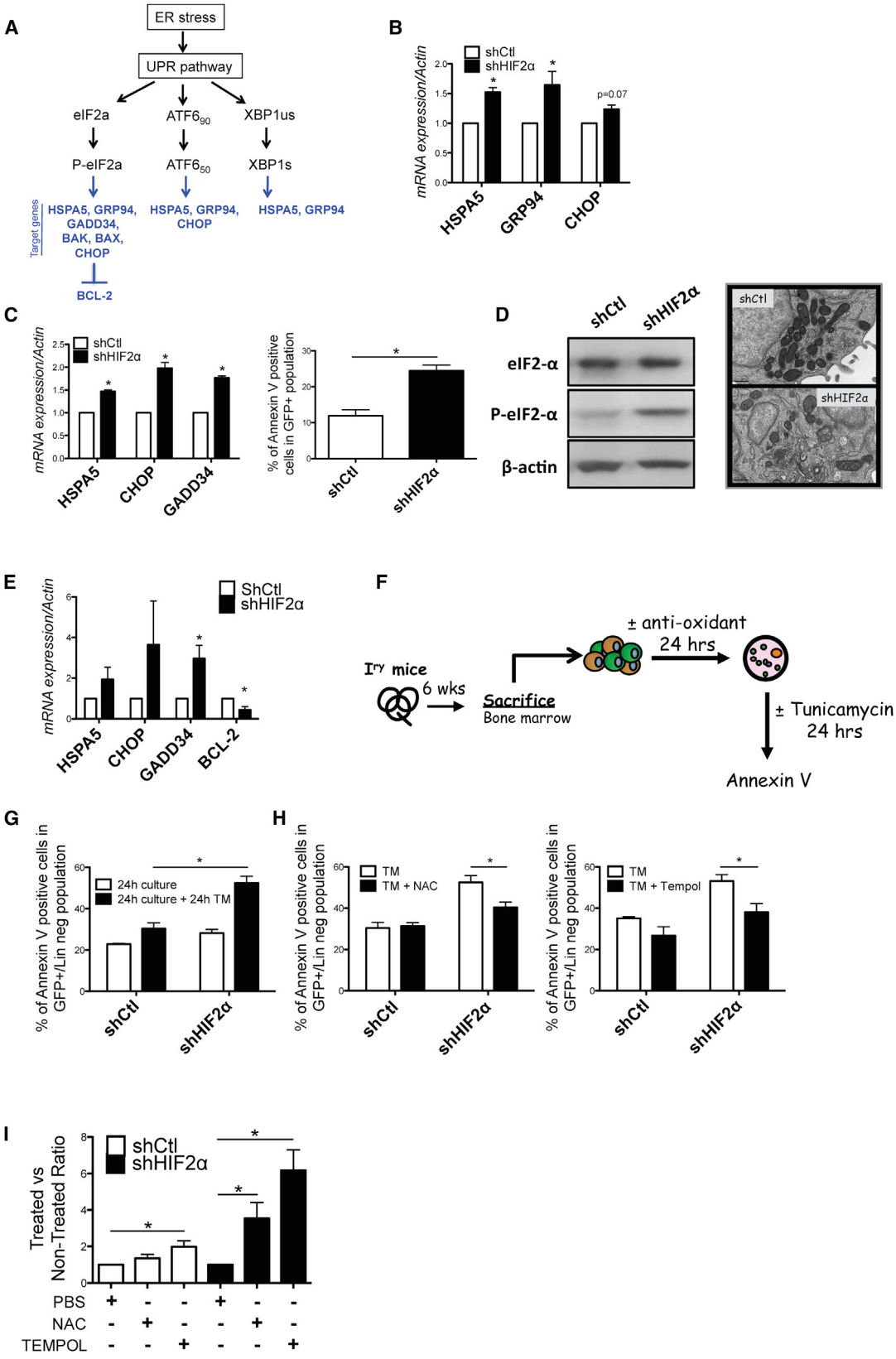

(legend on next page)

DISCUSSION

HSPCs reside in hypoxic niches in the BM where low oxygen levels play a key role in their maintenance. In the current report, we investigated the role of HIF transcription factors in human HSPCs. By knocking down HIF-1α and HIF-2α, we report that HIF-2α, and to a lesser extend HIF-1α, plays a major role in the regulation and maintenance of human HSPCs.

In vitro assays show that HIF-1α and HIF-2α are not required for the production of human progenitors engaged in the myeloid lineage since both HIF-1α- and HIF-2α-deficient myeloid cells were able to form colonies (Figure 2A). This is in agreement with the observations made in the *Hif-1α*-deficient mouse models, where *Hif-1α*-deficient cells are still competent at generating CFU-Cs in vitro and CFU-Ss (12 days) after transplantation (Takubo et al., 2010). Likewise, *Hif-2α* KO mouse BM cells produce normal CFU-Ss (8 days) (Scortegagna et al., 2003b).

In short-term repopulating assays (6 weeks posttransplant), we saw a significant decrease in hCD45$^+$GFP$^+$ cells engrafted in the shHIF1α group and an even sharper drop in the shHIF2α group (Figures 2D and 3B). This decrease was not due to a defect in homing (Figure 2E). Based on the facts that at 1 week posttransplant no difference in engraftment between control and shHIF2α cells could be detected, and that our intravital imaging does not show any difference in positioning 4 days posttransplant, we ruled out a possible effect on the "niche anchorage" of at least the shHIF2α cells in their microenvironment. Looking at long-term engraftment, there was a clear difference between the effect of HIF1α and HIF2α KD, where no further reduction of human engraftment was seen after 12 weeks in the shHIF1α group. This was further confirmed by the percentage of CD34$^+$CD38$^-$ present in the mice 24 weeks posttransplant, which was unchanged in shHIF1α as compared to the control group (Figure 3F) and the nonsignificant reduction in the engraftment after secondary transplantation (Figure 3G). Contrary to the conditional *Hif-1α* KO mouse model, where the only significant defect was observed in long-term repopulating capacity after serial transplantation, we established that the downregulation of HIF-1α in human HSPCs does not significantly affect the long-term self-renewing multilineage repopulating cells. However, it is possible that this is due to the compensatory upregulation of *HIF-2α* observed in shHIF1α-transduced cells (Figure S2C). This is also supported by the observation that *HES-1*, a target gene of HIF-2α, is upregulated in HIF-1α KD cells (Figure 1D).

It appears, however, that HIF-2α has a major effect in the maintenance of human HSPCs. Both short-term and long-term repopulating cells were significantly decreased, with a particularly sharp decrease in the HSPC compartment 24 weeks posttransplant and a reduction in the secondary transplantation capacity. We further show that this effect was due, at least in part, to an increase in ROS production, which correlates with a decrease in the expression of *SOD2* and *FXN*, genes involved in the cellular response to oxidative stress and in the maintenance of mitochondrial homeostasis. High levels of oxidative stress and increased levels of ROS have been previously reported in *Hif-2α*$^{-/-}$ mice (Scortegagna et al., 2003a) and in *Meis1*$^{-/-}$ HSCs, known to downregulate *Hif-2α* (Kocabas et al., 2012; Scortegagna et al., 2003a). HIF-2α has also been shown to regulate the expression of both *Fxn* and *Sod2* in mouse liver, where deletion of these genes results in mitochondrial disease (Oktay et al., 2007; Scortegagna et al., 2003a).

We show that in the BM, HSPCs silenced for HIF-2α have an increase in ROS production, which increases ER stress and activates the UPR pathway, the machinery that mediates the regulation of ER stress. Indeed, we could detect the upregulation of two downstream effectors, CHOP and GADD34 of the PERK signal transducer pathway, as well as upregulation of GRP94 and HSPA5. The UPR is a survival response to reduce the accumulation of unfolded proteins and to restore ER function. This adaptive response of the cells is characterized by a decrease in proliferation and protein synthesis. When ER stress cannot be mitigated and homeostasis cannot be reestablished, prolonged activation of the UPR pathway (here under continuous HIF-2α KD) results in the activation of cell death (review in Tabas and Ron, 2011; Rutkowski and Hegde, 2010; Walter and Ron, 2011). Our experiments show that HIF-2α KD HSPCs cultured

Figure 6. Increase in ROS in HIF-2α KD Induces ER Stress, Triggering Apoptosis

(A) Schematic overview of the UPR pathway.

(B) RT-QPCR of *HSPA5*, *CHOP*, and *GADD34* expression in CD34$^+$ cells transduced with shCtl or shHIF2α. B-ACTIN was used as control (n = 3). The results are expressed in comparison to the level of shCtl.

(C) Left panel, same as (B) but cells were treated for 24 hr with TM prior to mRNA extraction. Right panel, transduced shCtl and shHIF2α CD34$^+$ cells were cultured for 6 days and received 24 hr of TM treatment before apoptosis was assessed. Data represent the percentage of Annexin V$^+$ cells in the DAPI$^-$ population. Results are shown as the mean ± SEM. *p < 0.05.

(D) Left panel, eIF2α, p-eIF2α, and B-ACTIN protein expression in CD34$^+$ cells 8 days after transduction. CD34$^+$ were transduced with shCtl or shHIF2α, sorted on day 4 based on GFP$^+$, and cultured for another 4 days. Six hours before protein extraction cells were treated with TM. Right panel, electron microscopy on HIF-2α KD CD34$^+$ after 6 days in short-term liquid culture. Electron microscopy identifies features of ER stress, showed by the dilatation of the ER in the HIF-2α KD cells compared to control cells.

(E) RT-QPCR for *HSPA5*, *CHOP*, *GADD34*, and *BCL-2* expression in CD45$^+$GFP$^+$ human cells. Transduced CD45$^+$/GFP$^+$ cells were sorted from mice 6 weeks posttransplantation. Gene expression was normalized to *B-ACTIN* and then to the shCtl (n = 4). Results are shown as the mean ± SEM. *p < 0.05.

(F) Schematic representation of the experiment. Six weeks after transplantation, mice were sacrificed and BM from shCtl and shHIF2α mice was incubated for 24 hr in the presence or absence of NAC or TEMPOL before mice were treated with BM TM for another 24 hr. Early apoptosis was assessed before and after TM treatment. (shCtl, n = 5; shHIF-2α, n = 11.)

(G) Data represents the percentage of AnnexinV$^+$ cells in the DAPI$^-$ population. Results are shown as the mean ± SEM. *p < 0.05.

(H) TM-induced apoptosis was rescued in presence of NAC (left panel) or TEMPOL (right panel). Results are shown as the mean ± SEM. *p < 0.05.

(I) Mice were transplanted with CD34$^+$ cells transduced with either shCtl or shHIF2α and treated for 6 weeks with PBS, NAC, or TEMPOL. Results are shown as a percentage of GFP$^+$ cells in the human engraftment normalized to 100% GFP at day 4 and then to PBS-treated mice. ShCtl-PBS, n = 5; ShCtl-NAC, n = 4; ShCtl-TEMPOL, n = 5; shHIF2α-PBS, n = 4; shHIF2α-NAC, n = 5; shHIF2α-TEMPOL, n = 6. Results are shown as mean ± SEM. *p < 0.05.

See also Figure S4.

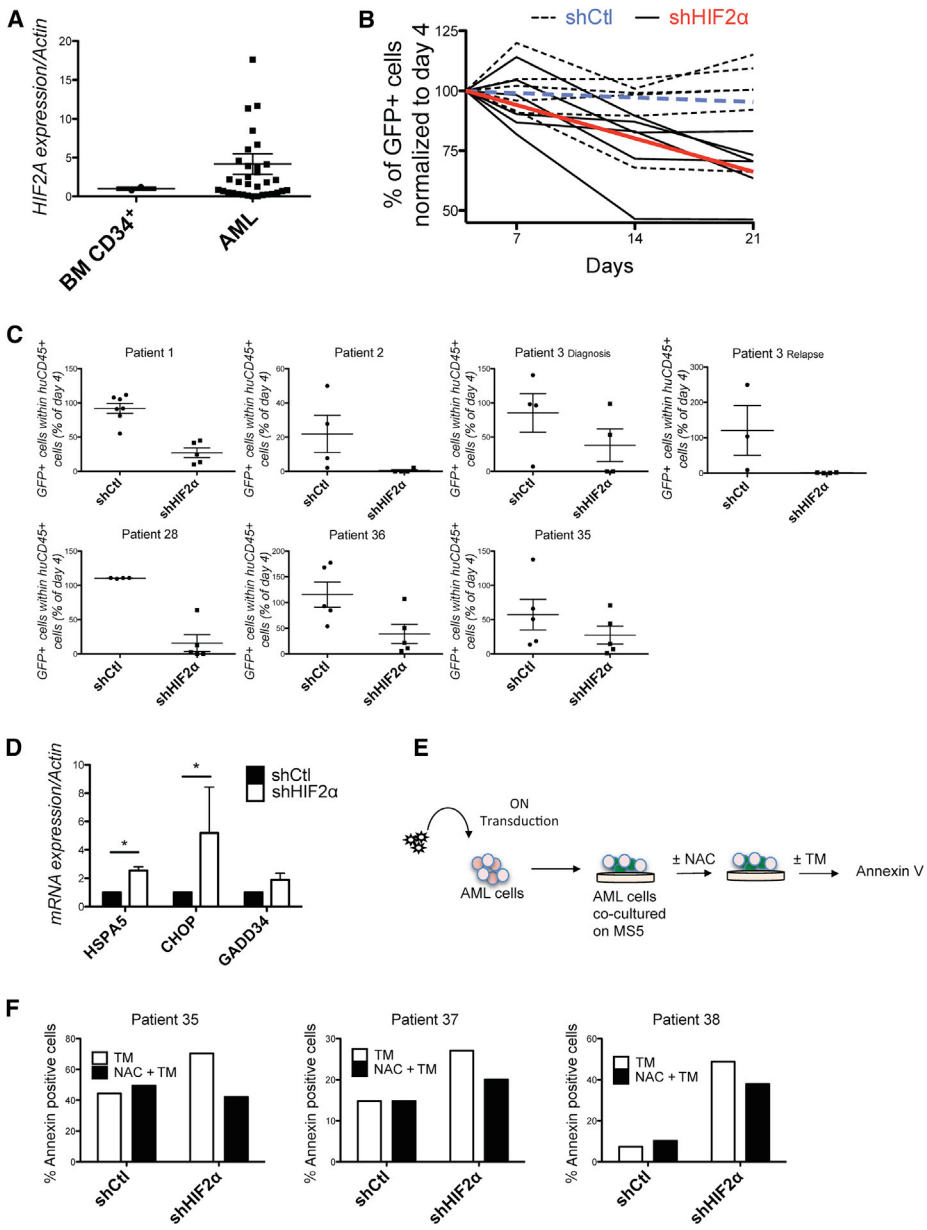

Figure 7. HIF-2α KD Impairs the Proliferation of Human Primary AML Cells

(A) Expression levels of *HIF-2α* in AML cells compared to normal adult BM CD34$^+$ cells. *B-ACTIN* was used as control (BM CD34$^+$ cells, n = 2; AML samples, n = 33). Results are shown as mean ± SEM.

(B) Cell growth of five AML samples transduced with shCtl or shHIF-2α and cocultured on MS5 cells for 3 weeks. Data represent the percentage of GFP$^+$ cells in hCD45-AML cells during the culture period. Results are shown as normalized to day 4 (100% GFP$^+$). Blue and red lines represent the mean of the five AML patient samples transduced with shCtl or shHIF2α, respectively. Overall $p < 0.007$.

(C) AML cells were transduced with shCtl or shHIF-2α and then injected into mice. Human graft was determined 12 weeks posttransplantation. Percentage of GFP$^+$ cells in the human graft normalized to day 4 (100% GFP$^+$) is presented. Results represent one or two independent experiments and each dot represents one mouse. Results are shown as mean ± SEM. Overall $p < 0.001$.

(D) RT-QPCR of *HSPA5*, *CHOP*, and *GADD34* expression in CD45$^+$/GFP$^+$ AML cells transduced with shCtl or shHIF2α and treated for 24 hr with TM prior to mRNA extraction. *B-ACTIN* was used as control. n = 4 AML patient samples. Results are shown as mean ± SEM. *$p < 0.05$.

(E) Schematic representation of the experiment. Two weeks after transduction, AML cells were incubated for 24 hr in the presence or absence of NAC and then for 24 hr with TM.

(F) Apoptosis was assessed on shCtl and shHIF2α transduced AML samples 24 hr before and after TM treatment. Data represents the percentage of AnnexinV$^+$ cells in the DAPI$^-$ population.

See also Figure S5.

in vitro present defects in proliferation. These defects cannot be explained by an increase in apoptosis, suggesting that cells may be in the adaptive phase of the UPR pathway where they try to restore ER functioning. However, in vivo, HIF-2α KD impairs long-term engraftment of HSPCs, suggesting a defect in cell survival probably due to high levels of ER stress. In agreement with that, our data demonstrate that HIF-2α-silenced cells (both in vitro and ex vivo) are more susceptible to apoptosis when they are under high levels of stress (i.e., when cells are treated with a potent ER stress inducer like TM). This suggests that HSPCs in the BM may be exposed to different stressors that, in conjunction with the increase in ROS production caused by HIF-2α KD, increase ER stress and make the cells undergo apoptosis through the UPR pathway. Based on the multifactorial effect of HIF-2α, it is possible that other pathways not described here are also involved.

We show that the increase in apoptosis after TM treatment was rescued by pretreating the cells with an antioxidant agent, like NAC or TEMPOL, both ex vivo and in vivo, demonstrating that ROS is upstream of the ER stress and UPR pathway in HSPCs. The same activation of the ER stress by ROS has been reported before in epithelial cells where cadmium caused ER stress via generation of ROS and ultimately apoptosis (Yokouchi et al., 2008).

We further demonstrate that the role of HIF-2α is not limited to the normal regulation of HSPCs and show that the KD of HIF-2α is also able to impede primary AML cells both ex vivo and in vivo by using the same UPR pathway. In glioblastoma, it has been shown recently that HIF-2α and multiple HIF-regulated genes are preferentially expressed in glioma stem cells (GSCs) in comparison to nonstem tumor cells and normal neural progenitors. Targeting both HIF-α subunits in GSCs inhibits self-renewal, proliferation, and survival in vitro and attenuates tumor-initiating potential of GSCs in vivo (Li et al., 2009). In AML, Wang et al. (2011) have reported that HIF-1α seems to be restricted to the $CD34^{+}CD38^{-}$ fraction enriched in leukemic stem cells (LSCs) and not in non-LSCs. Importantly, using the HIF-inhibitor echinomycin, they showed an efficient eradication of serially transplantable human AML in xenogenic models by preferential elimination of LSCs. Based on the data reported here, it is arguable that at least part of the effect of echinomycin treatment might have been through HIF-2α downregulation. Although further studies are needed, it is tempting to speculate that LSCs in AML might use enhanced expression of HIF-2α to protect them from oxidative stress. Therefore HIF-2α inhibition could still be proposed as a therapeutic target in the context of AML patients with enhanced ER stress, which would make them more prone to apoptosis. This could only work within a specific time window if the effect of silencing HIF-2α is more pronounced in AML LSCs than in normal HSCs, which will need to be further evaluated using potential HIF inhibitors.

All together, our data demonstrate the important regulatory role of HIF-2α in human hematopoiesis, in both normal and malignant conditions.

EXPERIMENTAL PROCEDURES

Generation of Lentiviral Vectors and Viral Particles

Twenty-one bp sense and antisense oligonucleotides were designed in the 3′-coding region of the human HIF-1α and HIF-2α genes. *HIF-1β* siRNA sequence was purchased from Thermo Scientific, UK (Figure S1). DNA fragments (Eurogentec, Angers, France) were cloned in the pic20-plasmid behind the polymerase III H1 promoter. H1-shRNA sequences were subcloned in the lentivirus (pTripΔU3Ef1α-EGFPMCSΔU3) that contains the enhanced GFP (eGFP) gene under the control of the EF1α promoter. An shRNA directed against the dsRed fluorescent protein (RFP) was used as a control (shCtl). Lentiviral supernatants were produced by transient $CaCl_2$ transfection of HEK293T cells. The viral titers measured on HEK293T cells by FACS (on eGFP expression),were 0.5×10^9 to 2×10^9 infectious particles/ml.

Source of Primary Human HSPCs and AML

UCB samples were obtained from normal full-term deliveries after signed informed consent. AML samples were obtained after informed consent at St Bartholomew's Hospital (London, UK). Both protocols were approved by the East London Ethical Committee and in accordance with the Declaration of Helsinki. AML samples were collected at diagnosis (n = 37) or relapse (n = 1). Details of patient samples are listed in Table S1.

Please refer to Supplemental Experimental Procedures for the remaining methodologies, materials, and reagents used with this manuscript.

ACCESSION NUMBERS

Microarray data are available at GEO database under accession number GSE49897.

SUPPLEMENTAL INFORMATION

Supplemental Information for this article includes Supplemental Experimental Procedures, five figures and two tables and can be found with this article online at http://dx.doi.org/10.1016/j.stem.2013.08.011.

AUTHOR CONTRIBUTIONS

F.M., K.R.P., and L.L.O. designed and performed the experiments, analyzed the data, and wrote the paper; K.F. and F.A.A. performed some experiments, analyzed the data, and provided constructive comments; H.R.R., I.L.G., and M.S.S. performed some experiments;R.M. performed the bioinformatics analysis of the microarray; Z.I. and H.V. analyzed the data; J.G. and D.T. provided the AML samples, information on the patients, and constructive comments on the paper; and D.B. designed the experiments, analyzed the data, and wrote the paper.

ACKNOWLEDGMENTS

The authors extend their thanks to all the staff at the Maison de Santé Protestante de Bordeaux-Bagatelle (Bordeaux, France), to Ms Besky at the Royal London Hospital for providing cord blood samples, and to the laboratory of virology headed by Professor Fleury. The authors are grateful to the Biological Resource Units, B. Rousseau (University of Bordeaux) for his valuable expertise, Dr. V. Pitard and the Flow Cytometry core facility members at LRI, and Gavin Kelly of the Bioinformatics Department at LRI for their expertise in sorting and statistical analysis. We would also like to thanks the electron microscopy core facility members at LRI for their help. This work was funded in part by Cancer Research UK to D.B. and by the COST Action TD0901 to FM. K.R.P. was financed in part by a grant from the French Ministère de l'Enseignement Supérieur et de la Recherche (MESR) and by Cancer Research UK; L.L.O., by a Marie Curie fellowship; and M.S.S. by a fellowship from the French Association of Cancer Research (ARC).

Received: December 5, 2012
Revised: July 9, 2013
Accepted: August 22, 2013
Published: October 3, 2013

REFERENCES

Adelman, D.M., Maltepe, E., and Simon, M.C. (1999). Multilineage embryonic hematopoiesis requires hypoxic ARNT activity. Genes Dev. *13*, 2478–2483.

Ang, S.O., Chen, H., Hirota, K., Gordeuk, V.R., Jelinek, J., Guan, Y., Liu, E., Sergueeva, A.I., Miasnikova, G.Y., Mole, D., et al. (2002). Disruption of oxygen homeostasis underlies congenital Chuvash polycythemia. Nat. Genet. *32*, 614–621.

Bertout, J.A., Majmundar, A.J., Gordan, J.D., Lam, J.C., Ditsworth, D., Keith, B., Brown, E.J., Nathanson, K.L., and Simon, M.C. (2009). HIF2alpha inhibition promotes p53 pathway activity, tumor cell death, and radiation responses. Proc. Natl. Acad. Sci. USA *106*, 14391–14396.

Ceradini, D.J., Kulkarni, A.R., Callaghan, M.J., Tepper, O.M., Bastidas, N., Kleinman, M.E., Capla, J.M., Galiano, R.D., Levine, J.P., and Gurtner, G.C. (2004). Progenitor cell trafficking is regulated by hypoxic gradients through HIF-1 induction of SDF-1. Nat. Med. *10*, 858–864.

Covello, K.L., Kehler, J., Yu, H., Gordan, J.D., Arsham, A.M., Hu, C.J., Labosky, P.A., Simon, M.C., and Keith, B. (2006). HIF-2alpha regulates Oct-4: effects of hypoxia on stem cell function, embryonic development, and tumor growth. Genes Dev. *20*, 557–570.

Danet, G.H., Pan, Y., Luongo, J.L., Bonnet, D.A., and Simon, M.C. (2003). Expansion of human SCID-repopulating cells under hypoxic conditions. J. Clin. Invest. *112*, 126–135.

Giuntoli, S., Rovida, E., Gozzini, A., Barbetti, V., Cipolleschi, M.G., Olivotto, M., and Dello Sbarba, P. (2007). Severe hypoxia defines heterogeneity and selects highly immature progenitors within clonal erythroleukemia cells. Stem Cells *25*, 1119–1125.

Gordan, J.D., Thompson, C.B., and Simon, M.C. (2007). HIF and c-Myc: sibling rivals for control of cancer cell metabolism and proliferation. Cancer Cell *12*, 108–113.

Gruber, M., Hu, C.J., Johnson, R.S., Brown, E.J., Keith, B., and Simon, M.C. (2007). Acute postnatal ablation of Hif-2alpha results in anemia. Proc. Natl. Acad. Sci. USA *104*, 2301–2306.

Hermitte, F., Brunet de la Grange, P., Belloc, F., Praloran, V., and Ivanovic, Z. (2006). Very low O2 concentration (0.1%) favors G0 return of dividing CD34+ cells. Stem Cells *24*, 65–73.

Hickey, M.M., Lam, J.C., Bezman, N.A., Rathmell, W.K., and Simon, M.C. (2007). von Hippel-Lindau mutation in mice recapitulates Chuvash polycythemia via hypoxia-inducible factor-2alpha signaling and splenic erythropoiesis. J. Clin. Invest. *117*, 3879–3889.

Jang, Y.Y., and Sharkis, S.J. (2007). A low level of reactive oxygen species selects for primitive hematopoietic stem cells that may reside in the low-oxygenic niche. Blood *110*, 3056–3063.

Keith, B., Johnson, R.S., and Simon, M.C. (2012). HIF1α and HIF2α: sibling rivalry in hypoxic tumour growth and progression. Nat. Rev. Cancer *12*, 9–22.

Kirito, K., Fox, N., Komatsu, N., and Kaushansky, K. (2005). Thrombopoietin enhances expression of vascular endothelial growth factor (VEGF) in primitive hematopoietic cells through induction of HIF-1alpha. Blood *105*, 4258–4263.

Kocabas, F., Zheng, J., Thet, S., Copeland, N.G., Jenkins, N.A., DeBerardinis, R.J., Zhang, C., and Sadek, H.A. (2012). Meis1 regulates the metabolic phenotype and oxidant defense of hematopoietic stem cells. Blood *120*, 4963–4972.

Kranc, K.R., Schepers, H., Rodrigues, N.P., Bamforth, S., Villadsen, E., Ferry, H., Bouriez-Jones, T., Sigvardsson, M., Bhattacharya, S., Jacobsen, S.E., and Enver, T. (2009). Cited2 is an essential regulator of adult hematopoietic stem cells. Cell Stem Cell *5*, 659–665.

Kubota, Y., Takubo, K., and Suda, T. (2008). Bone marrow long label-retaining cells reside in the sinusoidal hypoxic niche. Biochem. Biophys. Res. Commun. *366*, 335–339.

Lapidot, T., and Kollet, O. (2002). The essential roles of the chemokine SDF-1 and its receptor CXCR4 in human stem cell homing and repopulation of transplanted immune-deficient NOD/SCID and NOD/SCID/B2m(null) mice. Leukemia: official journal of the Leukemia Society of America. Leukemia Research Fund, UK *16*, 1992–2003.

Lévesque, J.P., Winkler, I.G., Hendy, J., Williams, B., Helwani, F., Barbier, V., Nowlan, B., and Nilsson, S.K. (2007). Hematopoietic progenitor cell mobilization results in hypoxia with increased hypoxia-inducible transcription factor-1 alpha and vascular endothelial growth factor A in bone marrow. Stem Cells *25*, 1954–1965.

Li, L., and Xie, T. (2005). Stem cell niche: structure and function. Annu. Rev. Cell Dev. Biol. *21*, 605–631.

Li, Z., Bao, S., Wu, Q., Wang, H., Eyler, C., Sathornsumetee, S., Shi, Q., Cao, Y., Lathia, J., McLendon, R.E., et al. (2009). Hypoxia-inducible factors regulate tumorigenic capacity of glioma stem cells. Cancer Cell *15*, 501–513.

Liu, Y.L., Yu, J.M., Song, X.R., Wang, X.W., Xing, L.G., and Gao, B.B. (2006). Regulation of the chemokine receptor CXCR4 and metastasis by hypoxia-inducible factor in non small cell lung cancer cell lines. Cancer Biol. Ther. *5*, 1320–1326.

Malhotra, J.D., and Kaufman, R.J. (2007). The endoplasmic reticulum and the unfolded protein response. Semin. Cell Dev. Biol. *18*, 716–731.

Miharada, K., Karlsson, G., Rehn, M., Rörby, E., Siva, K., Cammenga, J., and Karlsson, S. (2011). Cripto regulates hematopoietic stem cells as a hypoxic-niche-related factor through cell surface receptor GRP78. Cell Stem Cell *9*, 330–344.

Morrison, S.J., and Spradling, A.C. (2008). Stem cells and niches: mechanisms that promote stem cell maintenance throughout life. Cell *132*, 598–611.

Oktay, Y., Dioum, E., Matsuzaki, S., Ding, K., Yan, L.J., Haller, R.G., Szweda, L.I., and Garcia, J.A. (2007). Hypoxia-inducible factor 2alpha regulates expression of the mitochondrial aconitase chaperone protein frataxin. J. Biol. Chem. *282*, 11750–11756.

Orkin, S.H., and Zon, L.I. (2008). Hematopoiesis: an evolving paradigm for stem cell biology. Cell *132*, 631–644.

Parmar, K., Mauch, P., Vergilio, J.A., Sackstein, R., and Down, J.D. (2007). Distribution of hematopoietic stem cells in the bone marrow according to regional hypoxia. Proc. Natl. Acad. Sci. USA *104*, 5431–5436.

Pedersen, M., Löfstedt, T., Sun, J., Holmquist-Mengelbier, L., Påhlman, S., and Rönnstrand, L. (2008). Stem cell factor induces HIF-1alpha at normoxia in hematopoietic cells. Biochem. Biophys. Res. Commun. *377*, 98–103.

Piccoli, C., D'Aprile, A., Ripoli, M., Scrima, R., Boffoli, D., Tabilio, A., and Capitanio, N. (2007). The hypoxia-inducible factor is stabilized in circulating hematopoietic stem cells under normoxic conditions. FEBS Lett. *581*, 3111–3119.

Pietras, A., Hansford, L.M., Johnsson, A.S., Bridges, E., Sjölund, J., Gisselsson, D., Rehn, M., Beckman, S., Noguera, R., Navarro, S., et al. (2009). HIF-2alpha maintains an undifferentiated state in neural crest-like human neuroblastoma tumor-initiating cells. Proc. Natl. Acad. Sci. USA *106*, 16805–16810.

Qing, G., and Simon, M.C. (2009). Hypoxia inducible factor-2alpha: a critical mediator of aggressive tumor phenotypes. Curr. Opin. Genet. Dev. *19*, 60–66.

Rezvani, H.R., Dedieu, S., North, S., Belloc, F., Rossignol, R., Letellier, T., de Verneuil, H., Taïeb, A., and Mazurier, F. (2007). Hypoxia-inducible factor-1alpha, a key factor in the keratinocyte response to UVB exposure. J. Biol. Chem. *282*, 16413–16422.

Rutkowski, D.T., and Hegde, R.S. (2010). Regulation of basal cellular physiology by the homeostatic unfolded protein response. J. Cell Biol. *189*, 783–794.

Ryan, H.E., Lo, J., and Johnson, R.S. (1998). HIF-1 alpha is required for solid tumor formation and embryonic vascularization. EMBO J. *17*, 3005–3015.

Scadden, D.T. (2006). The stem-cell niche as an entity of action. Nature *441*, 1075–1079.

Scortegagna, M., Ding, K., Oktay, Y., Gaur, A., Thurmond, F., Yan, L.J., Marck, B.T., Matsumoto, A.M., Shelton, J.M., Richardson, J.A., et al. (2003a). Multiple organ pathology, metabolic abnormalities and impaired homeostasis of reactive oxygen species in Epas1-/- mice. Nat. Genet. *35*, 331–340.

Scortegagna, M., Morris, M.A., Oktay, Y., Bennett, M., and Garcia, J.A. (2003b). The HIF family member EPAS1/HIF-2alpha is required for normal hematopoiesis in mice. Blood *102*, 1634–1640.

Semenza, G.L. (2009a). HIF-1 inhibitors for cancer therapy: from gene expression to drug discovery. Curr. Pharm. Des. *15*, 3839–3843.

Semenza, G.L. (2009b). Involvement of oxygen-sensing pathways in physiologic and pathologic erythropoiesis. Blood *114*, 2015–2019.

Simsek, T., Kocabas, F., Zheng, J., Deberardinis, R.J., Mahmoud, A.I., Olson, E.N., Schneider, J.W., Zhang, C.C., and Sadek, H.A. (2010). The distinct metabolic profile of hematopoietic stem cells reflects their location in a hypoxic niche. Cell Stem Cell *7*, 380–390.

Tabas, I., and Ron, D. (2011). Integrating the mechanisms of apoptosis induced by endoplasmic reticulum stress. Nat. Cell Biol. *13*, 184–190.

Takubo, K., Goda, N., Yamada, W., Iriuchishima, H., Ikeda, E., Kubota, Y., Shima, H., Johnson, R.S., Hirao, A., Suematsu, M., and Suda, T. (2010). Regulation of the HIF-1alpha level is essential for hematopoietic stem cells. Cell Stem Cell *7*, 391–402.

Walter, P., and Ron, D. (2011). The unfolded protein response: from stress pathway to homeostatic regulation. Science *334*, 1081–1086.

Wang, Y., Liu, Y., Malek, S.N., Zheng, P., and Liu, Y. (2011). Targeting HIF1α eliminates cancer stem cells in hematological malignancies. Cell Stem Cell *8*, 399–411.

Yokouchi, M., Hiramatsu, N., Hayakawa, K., Okamura, M., Du, S., Kasai, A., Takano, Y., Shitamura, A., Shimada, T., Yao, J., and Kitamura, M. (2008). Involvement of selective reactive oxygen species upstream of proapoptotic branches of unfolded protein response. J. Biol. Chem. *283*, 4252–4260.

Yoon, D., Pastore, Y.D., Divoky, V., Liu, E., Mlodnicka, A.E., Rainey, K., Ponka, P., Semenza, G.L., Schumacher, A., and Prchal, J.T. (2006). Hypoxia-inducible factor-1 deficiency results in dysregulated erythropoiesis signaling and iron homeostasis in mouse development. J. Biol. Chem. *281*, 25703–25711.